*Original Article*

# Mandibular and glenoid fossa changes after bone-anchored maxillary protraction therapy in patients with UCLP: *A 3-D preliminary assessment*

**Marilia Yatabe[a]; Daniela Garib[b]; Renato Faco[c]; Hugo de Clerck[d]; Bernardo Souki[e]; Guilherme Janson[f]; Tung Nguyen[g]; Lucia Cevidanes[h]; Antonio Ruellas[i]**

## ABSTRACT

**Objective:** To assess mandibular and glenoid fossa (GF) changes after bone-anchored maxillary protraction (BAMP) therapy in patients with unilateral complete cleft lip and palate (UCLP).

**Materials and Methods:** The cleft group (CG) comprised 19 patients with (mean initial age of 11.8 years). The noncleft group (NCG) comprised 24 patients without clefts (mean initial age of 11.7 years). Both groups had Class III malocclusion and were treated with BAMP therapy for 18 and 12 months, respectively. Cone-beam computed tomography (CBCT) exams were performed before and after treatment and superimposed on the anterior cranial fossa (ACF). Mandibular rotations and three-dimensional linear displacements of the mandible and GF were quantified. A *t*-test corrected for multiple testing (Holm-Bonferroni method) and a paired *t*-test were used to compare, respectively, the CG and NCG and cleft vs noncleft sides ($P < .05$).

**Results:** Immediately after active treatment, the GF was displaced posteriorly and laterally in both groups relative to the ACF. The overall GF changes in the CG were significantly smaller than in the NCG. Condylar displacement was similar in both groups, following a posterior and lateral direction. The gonial angle was displaced similarly posteriorly, laterally, and inferiorly in both groups. The intercondylar line rotated in opposite directions in the CG and NCG groups. In the CG, most changes of the GF and mandible were symmetrical.

**Conclusions:** Overall GF and mandibular changes after BAMP therapy were similar in patients with and without clefts. The exception was the posterior remodeling of the GF that was slightly smaller in patients with UCLP. (*Angle Orthod.* 2017;87:423–431)

**KEY WORDS:** Cleft lip; Cleft palate; Orthodontic anchorage procedure; Angle Class III

## INTRODUCTION

Craniofacial growth is severely compromised in patients with unilateral complete cleft lip and palate (UCLP).[1] Primary surgeries for lip and palate repair in this group contribute to deficient maxillary growth and a Class III skeletal pattern.[1] The maxilla is often positioned more superiorly and posteriorly in patients

[a] Postdoctoral Fellow, Hospital for Rehabilitation of Craniofacial Anomalies, University of São Paulo, Bauru-São Paulo, Brazil.

[b] Associate Professor, Department of Orthodontics, Bauru Dental School, Hospital for Rehabilitation of Craniofacial Anomalies, University of São Paulo, Bauru-São Paulo, Brazil.

[c] Maxillofacial Surgeon, Hospital for Rehabilitation of Craniofacial Anomalies, University of São Paulo, Bauru-São Paulo, Brazil.

[d] Visiting Professor, Department of Orthodontics, School of Dentistry, University of North Carolina, Chapel Hill, NC.

[e] Associate Professor, Department of Orthodontics, Pontifical Catholic University of Minas Gerais, Belo Horizonte, Minas Gerais, Brazil.

[f] Professor, Department of Orthodontics, Bauru Dental School, University of São Paulo, Bauru-São Paulo, Brazil.

[g] Associate Professor, Department of Orthodontics, School of Dentistry. University of North Carolina, Chapel Hill, NC.

[h] Associate Professor, Department of Orthodontics and Pediatric Dentistry, School of Dentistry, University of Michigan, Ann Arbor, Mich.

[i] Associate Professor, Department of Orthodontics, Federal University of Rio de Janeiro, Rio de Janeiro, Brazil.

Corresponding author: Dr Marilia Yatabe, Hospital for Rehabilitation of Craniofacial Anomalies, University of São Paulo, R. Silvio Marchione, 3-20, Vila Universitária, Bauru - SP, 17012-900, Brazil
(e-mail: marilia.yatabe@gmail.com)

Accepted: August 2016. Submitted: May 2016.
Published Online: September 26, 2016

**Table 1.** Sample Description

| | N (Cleft Side Right/Left) | Male/Female | Mean Age at T1 CBCT Exam | Wits Appraisal Mean (SD) |
|---|---|---|---|---|
| Cleft group (CG) | 19 (5/14) | 17/7 | 11.8 y (± 9 mo) | −7.13 (3.13) |
| Noncleft group (NCG) | 24 | 10/15 | 11.9 y (± 14 mo) | −4.8 (2.8) |

with UCLP compared with patients with incomplete cleft or no cleft. Additionally, patients with UCLP have vertical maxillary deficiency.[2]

Mandibular growth is less affected than is maxillary in the presence of UCLP, although individuals with UCLP demonstrate a slightly smaller and retruded mandible.[3] Mandibular growth is commonly hyperdivergent in UCLP with smaller ramus height, more obtuse gonial angles, and an increased lower anterior facial height.[2] These mandibular morphologies are seen in nonoperated and operated patients with UCLP and therefore are not influenced by the primary plastic surgeries.[4] Some authors suggest that the vertical mandibular pattern observed in patients with cleft lip and palate might be related to tongue position.[5] Constriction of the maxilla, along with lingually tipped incisors, forces the tongue to rest between the maxillary and mandibular teeth, increasing the freeway space.[5] This causes the mandible to overclose when in occlusion, giving the individual a prognathic and reduced facial height appearance.[5] Another hypothesis states that frequent mouth breathing and deviated septum may influence mandibular growth in UCLP, mainly at the gonial region.[6]

Facemask therapy is the most common Class III malocclusion treatment, and the main facial changes that occur include anterior displacement of the maxilla, backward rotation of the mandible, and increased lower anterior facial height.[7] Considering that patients with UCLP usually show a vertical growth pattern, clockwise rotation of the mandible during facemask therapy is an unfavorable effect.

Recently, new orthopedic therapy for Class III malocclusion has been described.[8] Treatment with bone-anchored maxillary protraction (BAMP) has allowed greater amounts of maxillary advancement coupled with better control of mandibular rotation. BAMP therapy produces a closure of the gonial angle and a slight restriction of the anterior displacement of the mandible in noncleft individuals.[9] Compared with the facemask, BAMP therapy, with better vertical control, does not result in clockwise rotation of the mandible.[9]

Few studies have reported that remodeling of the glenoid fossa (GF) occurs after mandibular orthopedic treatment: one is a magnetic resonance study after Herbst appliance therapy[10] and the other is a histologic study in rhesus monkeys treated with chincup therapy.[11] The only previous study performed after maxillary traction in humans showed a posterior remodeling of the anterior and posterior eminences of the GF.[12] However, GF and mandibular outcomes after BAMP therapy in patients with UCLP have not been evaluated. Therefore, the aim of this study is to evaluate and compare mandibular displacement and GF remodeling after maxillary protraction anchored in miniplates in patients with and without UCLP. The hypothesis is that no difference is observed between patients with and without CLP.

## MATERIALS AND METHODS

This retrospective study was approved by the Ethics Committee of the University of Michigan (IRB 19.693), Ann Arbor, MI.

The cleft group (CG) consisted of CBCT exams (FOV 13 × 16 cm, voxel 0.4 mm, 8.9 s) of 19 patients with UCLP and maxillary sagittal deficiency, treated consecutively at the Hospital for Rehabilitation of Craniofacial Anomalies, University of São Paulo. Inclusion criteria for the BAMP treatment were

- patient's age at the beginning of the treatment from 10 to 13 years old,
- mandibular permanent canines fully erupted,
- secondary alveolar bone graft performed at least 3 months before starting BAMP therapy,
- Goslon Yardstick[13] between 3 and 5.

Exclusion criteria were

- patients with syndromes or inadequate oral hygiene,
- treatment interruption,
- miniplate instability,
- CBCT with motion artifacts.

Mandibular displacement was performed in 12 out of the 19 patients with cleft because seven CBCT exams (T1/T2) were acquired with the mouth open. The comparison noncleft group (NCG) consisted of secondary data analysis[14] of 25 Class III noncleft patients. One patient of the NCG was excluded for missing data. The final samples are described in Table 1. Similar clinical protocol[8] was performed in both groups. CBCT exams were obtained before (T1) and after treatment (T2) with intervals of 18 and 12 months for CG and NCG, respectively.

To measure linear and angular D displacement, the following steps were taken:

1. Volumetric label map: Using ITK-SNAP (2.4).0

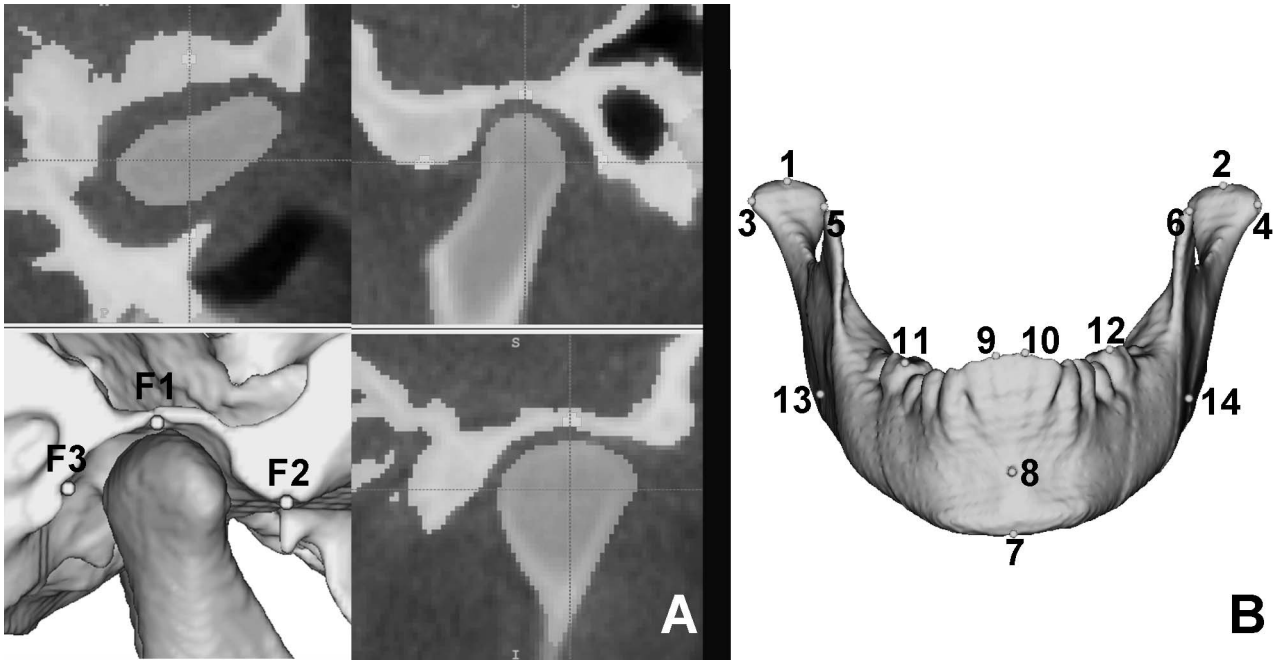


**Figure 1.** (A) Prelabeled anatomical points of the glenoid fossa (GF) over the grey scale scan in ITK-SNAP (2.4):[15] (F1) GF-Superior; (F2) GF-Anterior; (F3) GF-Posterior. (B) Yellow surface model of mandible created from the segmentation and, in red, anatomical landmarks placed on the 3-D surface model: (1, 2) condyle-superior (SC); (3, 5) condyle-lateral (CL); (4, 6) condyle-medial (MC); (7) menton (Me); (8) B-point (B); (9, 10) incisal edge of mandibular central incisors (L1); (11, 12) mesiobuccal cusp of permanent first molar (L6); (13, 14) gonion (Go).

(www.itksnap.org),[15] the cranial base, maxilla, and mandible were segmented for T1 and T2 scans (https://youtu.be/OunM2b_Hm-Y).

2. Virtual three-dimensional (3-D) surface model: Using the 3DSlicer-4.4 (www.slicer.org),[16] we created the virtual 3-D surface models from the T1 and T2 volumetric label maps (https://youtu.be/3bvaKY4fpns).
3. Head Orientation[17]: The 3DSlicer Software 4.4[16] displays a 3-D coordinate system that was kept fixed to be used as reference to consistently orient the 3-D models of all patients. Using axial, coronal, and sagittal views of the 3-D models, the T1 model was moved to match the midsagittal plane (defined by glabella, crista galli, and basion) vertically and coincident with the sagittal plane of the 3-D coordinate system. The Frankfurt horizontal plane was oriented to match the axial plane, and the horizontal infraorbitale (most inferior, anterior point of the left and right margins of the orbit) line was oriented to coincide with the coronal plane.
4. 3-D cranial base superimposition: The 3-D superimposition registered on the cranial base was performed in two steps: (a) Using the 3DSlicer 4.4,[16] the T2 scan was manually approximated to the T1-oriented scan (https://youtu.be/lDDsLLItCvs); (b) Using the anterior cranial fossa label map as a best-fit reference, a fully automated voxel-based registration was performed in the 3DSlicer 4.4 (https://youtu.be/sYaLAH_c4CQ).[16,18] The matrix generated from registration of T2 over T1 was applied to the T2 scan, volumetric label map, and 3-D surface model, also in the 3DSlicer 4.4.[16]
5. Landmark identification*:* (a) Anatomic points were defined at T1 and T2 using the gray scale image (multiplanar reconstruction) as reference using ITK-SNAP-2.4.0[15] (Figure 1a). (b) The volumetric point models were transformed into surface point models using the Slicer 4.4[16] (Figure 1b). (c) Landmarks were placed at T1 and T2 surface point models using the Q3DC tool in the 3DSlicer 4.4[16] as displayed in Figure 1b and detailed in Table 2.
6. Quantitative measurements: Using the Q3DC tool in the 3DSlicer 4.4[16] (https://youtu.be/TQjFEmA-baM), 3-D linear distances and the amount of directional changes in each plane of the 3-D space (X- [mediolateral], Y- [anteroposterior], and Z- [superior-inferior] axes, respectively) were measured between landmarks placed in the T1 and registered T2 surface models. Positive values represent anterior, inferior, and lateral displacements. Negative values represent posterior, superior, and medial displacements. Angular measurements were calculated between T2 and T1 (Figure 2, Table 2). Mandibular rotations were measured in a superior view (yaw), anterior view (roll), and sagittal view (pitch). Positive values represent clockwise (CW) rotation, and negative values represent counterclockwise (CCW)

**Table 2** Landmark Description and Line Identification

| Anatomical Landmark | Reference Number in Figures 1 and 2 | Description |
|---|---|---|
| Glenoid fossa-superior (FS) | F1 | Most superior and central point of superior curvature of glenoid fossa |
| Glenoid fossa-anterior (FA) | F2 | Middle point between most inferior point of anterior eminence of glenoid fossa and FS |
| Glenoid fossa-posterior | F3 | Middle point between most inferior point of posterior eminence of glenoid fossa and FS |
| Condyle-superior (CS) | 1 (right)/2 (left) | Most superior and central point of condyle |
| Condyle-lateral (CL) | 3 (right)/4 (left) | Most extreme point of lateral pole of condyle |
| Condyle-medial (CM) | 5 (right)/6 (left) | Most extreme point of medial pole of condyle |
| Menton (Me) | 7 | Most inferior point of chin |
| B-Point (B) | 8 | Most posterior point of anterior curvature of symphysis |
| Incisal of mandibular central incisor (I-L1) | 9 (right) / 10 (left) | Central point of each mandibular central incisor |
| Mandibular first permanent molar (L6) | 11 (right) / 12 (left) | Mesiobuccal cusp of mandibular first permanent molar |
| Gonion (Go) | 13 (right) / 14 (left) | Projection of a virtual bisector of a line adjacent to mandibular base and posterior border of mandible |
| Intercondylar line | Lines 1 and 3 | Orthogonal distance between right and left CS |
| Intermolar line | Lines 2 and 4 | Orthogonal distance between right and left L6 |
| Co-Me | Line 5 | Orthogonal distance between middle point of right and left CS with Me point |
| Occlusal line | Line 6 | Orthogonal distance between middle point of right and left L6 with middle point of right and left I-L1 |

rotation in the anterior and sagittal views. In a superior view, positive value represents a rotation to the right, and negative value, to the left. Semitransparent superimpositions of the mandible were used to visually demonstrate overall changes in the CG (Figure 3).

### Statistical Analysis

Intrarater correlation coefficients were performed to assess the reproducibility of linear and angular measurements between T1 and T2.

All variables showed a normal distribution. Statistical analysis was performed with SPSS Statistical Software Package (Version 21.0; SPSS, Chicago, Ill). Comparisons between the CG and NCG considering the mean value between right and left sides were performed using an independent *t*-test corrected for multiple testing (Holm-Bonferroni method). Comparisons between cleft sides (Cs) and noncleft sides (NCs) in the CG was performed using a paired *t*-test. Level of significance was 0.05.

## RESULTS

The ICCs for linear and angular measurements showed very good intraexaminer agreement (Table 3).

### Fossa Remodeling

Overall, the GF was displaced laterally, posteriorly, and inferiorly. No intergroup statistical difference was found in the three spatial planes (X, Y, and Z). However, the total linear displacement of fossa landmarks showed a significantly smaller magnitude

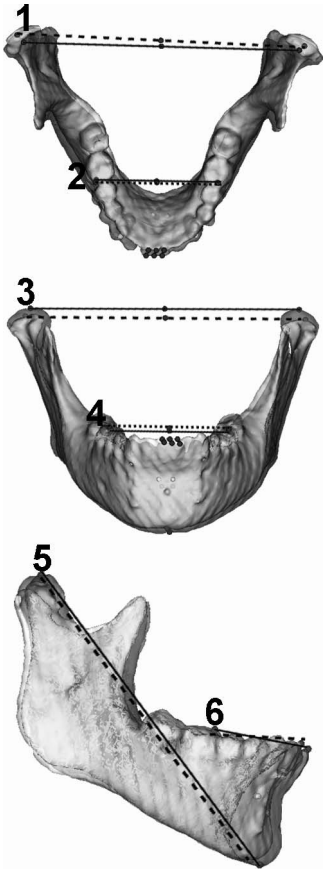


**Figure 2.** Yaw, roll, and pitch measurements. T1: black line; T2: dotted line. (1) Intercondylar line: yaw; (2) Intermolar line: yaw; (3) Intercondylar line: roll; (4) Intermolar line: roll; (5) Co-Me line: pitch; (6) Occlusal plane: pitch.

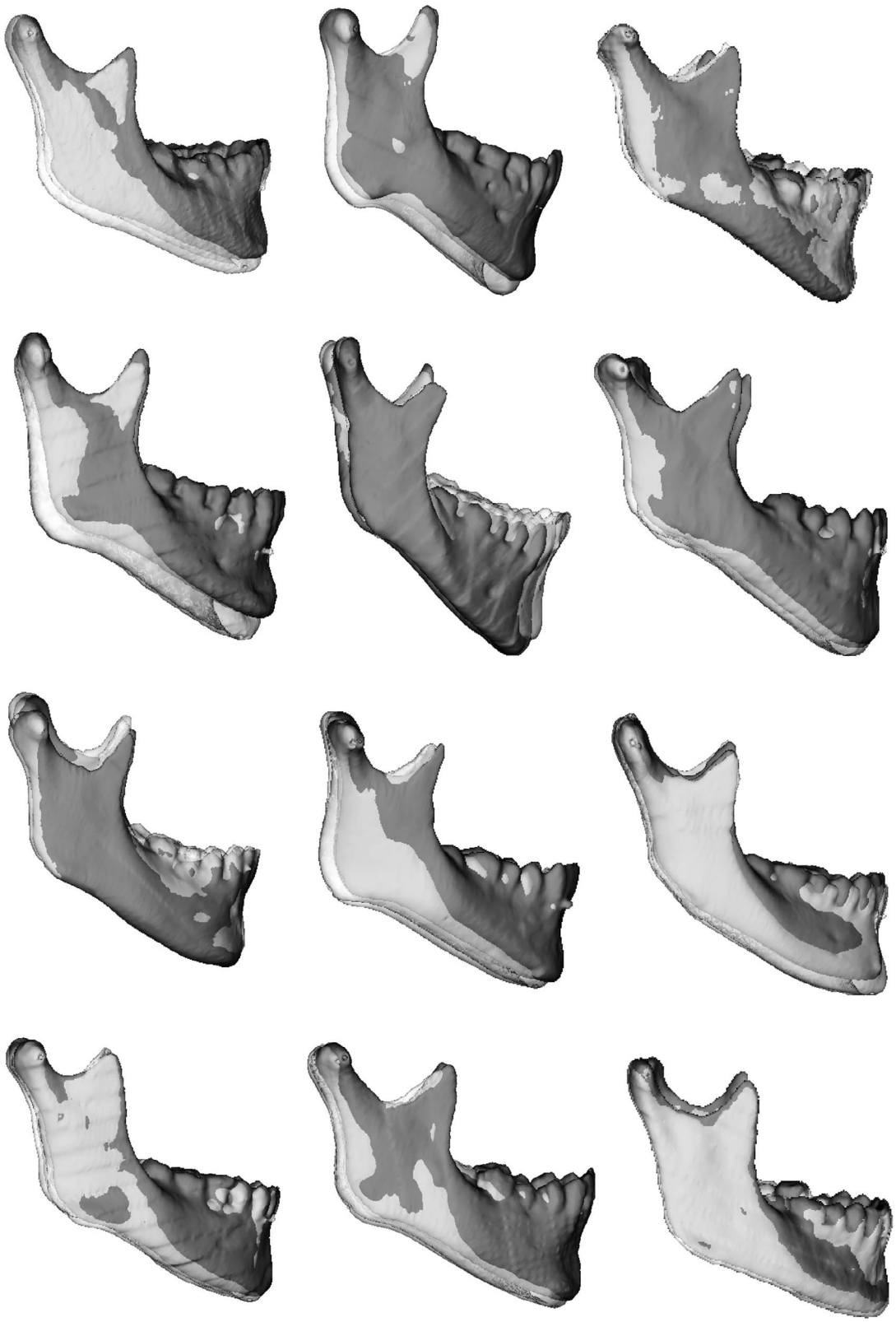

**Figure 3.** Lateral visualization of the semitransparent superimposition of T1 (green) and T2 (semitransparent white) mandibles of the CG.

**Table 3** ICC Results of Intraexaminer Agreement of Linear (mm) and Angular (°) Measurements

| | Mediolateral | Anteroposterior | Superior-inferior | 3-D | Average ICC |
|---|---|---|---|---|---|
| Linear measurements | | | | | |
| Superior condyle T1-T2 | 0.67 | 0.85 | 0.99 | 0.92 | 0.85 |
| Lateral pole T1-T2 | 0.91 | 0.85 | 0.91 | 0.77 | 0.86 |
| Medial pole T1-T2 | 0.91 | 0.84 | 0.92 | 0.88 | 0.88 |
| Menton T1-T2 | 0.72 | 0.80 | 0.79 | 0.83 | 0.79 |
| Point B T1-T2 | 0.68 | 0.96 | 0.72 | 0.82 | 0.80 |
| Incisal T1-T2 | 0.71 | 0.89 | 0.70 | 0.86 | 0.79 |
| 1st molar T1-T2 | 0.70 | 0.87 | 0.97 | 0.88 | 0.85 |
| Go T1-T2 | 0.74 | 0.77 | 0.83 | 0.86 | 0.80 |
| Angular measurements | Yaw | Roll | Pitch | | |
| Intercondylar angle | 0.67 | 0.9 | – | | |
| Intermolar angle | 0.86 | 0.81 | – | | |
| Occlusal line | – | – | 0.89 | | |
| Co-Me | – | – | 0.95 | | |

in the CG (Table 4). Right and left GF was symmetrically remodeled in the CG (Table 5).

### Mandibular Displacement

The rami and condyles were also displaced laterally, posteriorly, and inferiorly, symmetrically to the GF in both CG and NCG groups (Table 4). The only statistical differences found were the medial displacement of menton and I-L1 in the CG, while they displaced laterally in the NCG (Table 4).

When we compared Cs and NCs, no differences were found for either anteroposterior or superior-inferior displacements of any mandibular landmarks. The exception was the medial pole of the condyle, which showed a significantly larger lateral displacement on the Cs compared with the opposite side (Table 5).

### Mandibular Rotation

The only significant difference between the CG and NCG groups was found for the intercondylar line in the anterior view. The CG showed a slight CCW roll, while the NCG showed a CW roll (Table 6).

Semitransparency superimpositions of the mandibles are shown in Figure 3. GF, condylar, and temporomandibular changes of the patient with the largest amount of maxillary protraction are illustrated in Figure 4.

## DISCUSSION

This is the first study to assess and highlight mandibular and GF changes that occur with maxillary protraction therapy in patients with UCLP. These results

**Table 4** Descriptive and Statistical Analyses of the Comparison of Linear Measurements (T2–T1) between CG and NCG[a]

| | Anteroposterior (mm) | | | Mediolateral (mm) | | | Superior-inferior (mm) | | | 3-D Displacement (mm) | | |
|---|---|---|---|---|---|---|---|---|---|---|---|---|
| | Cg | NCg | *P* | Cg | NCg | *P* | Cg | NCg | *P* | Cg | NCg | *P* |
| Superior fossa | −0.49 (0.75) | −0.76 (0.94) | .333 | 0.59 (0.59) | 0.53 (0.94) | .799 | −0.06 (0.28) | 0.09 (0.69) | .360 | 1.34 (0.42) | 1.95 (0.68) | .001* |
| Anterior fossa | −0.24 (0.50) | −0.59 (0.99) | .155 | 0.68 (0.52) | 0.65 (1.06) | .895 | 0.12 (0.21) | 0.37 (0.70) | .115 | 1.18 (0.29) | 1.88 (0.71) | .000* |
| Posterior fossa | −0.53 (0.61) | −0.81 (0.83) | .213 | 0.62 (0.54) | 0.71 (1.04) | .733 | 0.12 (0.17) | 0.34 (0.69) | .140 | 1.31 (0.43 | 1.95 (0.64) | .000* |
| Superior condyle | −0.80 (0.69) | −1.00 (1.12) | .506 | 0.78 (0.88) | 0.85 (0.58) | .797 | −0.22 (0.47) | 0.24 (1.07) | .086 | 1.68 (0.70) | 2.11 (0.88) | .118 |
| Lateral condyle | −1.32 (0.79) | −0.93 (1.08) | .221 | 0.85 (0.57) | 0.82 (0.74) | .911 | 0.19 (0.88) | 0.55 (1.18) | .312 | 2.03 (0.79) | 2.26 (0.86) | .432 |
| Medial condyle | −0.99 (0.64) | −1.17 (1.01) | .513 | 0.38 (0.42) | 0.55 (0.49) | .275 | 0.13 (0.58) | 0.52 (1.07) | .163 | 1.62 (0.72) | 2.07 (0.83) | .104 |
| Menton | −1.46 (2.78) | −0.12 (2.57) | .267 | −0.70 (1.44) | 0.16 (1.06) | .046 | 1.68 (3.07) | 1.41 (2.70) | .802 | 4.22 (2.39) | 3.40 (2.25) | .382 |
| B-Point | −1.20 (2.35) | −0.19 (2.35) | .270 | −0.77 (1.39) | 0.16 (1.03) | .038* | 1.91 (3.94) | 1.16 (3.54) | .581 | 4.62 (2.41) | 3.83 (2.29) | .314 |
| Incisal L1 | 0.04 (1.92) | 0.25 (1.90) | .756 | −0.64 (0.88) | 0.27 (1.01) | .013* | 2.09 (3.06) | 0.61 (2.43) | .168 | 3.80 (1.87) | 2.86 (2.65) | .155 |
| Mesiobuccal cusp L6 | 0.22 (1.25) | 0.78 (2.05) | .316 | 0.07 (0.86) | 0.12 (0.76) | .864 | 2.42 (2.26) | 1.64 (1.77) | .307 | 3.43 (1.45) | 3.08 (1.62) | .522 |
| Gonion | −2.36 (2.70) | −2.03 (1.52) | .699 | 0.89 (0.76) | 0.85 (0.49) | .859 | 1.34 (1.54) | 1.70 (2.24) | .573 | 3.93 (2.11) | 3.74 (1.67) | .796 |

[a] CG indicates Cleft group; NCG, noncleft group.
* Statistically significant after Holm-Bonferroni correction for multiple comparisons.

**Table 5** Descriptive and Statistical Analyses of the Comparison of Linear Measurements (T2–T1) Between Cs x NCs[a]

| | Anteroposterior (mm) | | | Mediolateral (mm) | | | Superior-inferior (mm) | | | 3-D Displacement (mm) | | |
|---|---|---|---|---|---|---|---|---|---|---|---|---|
| | Cs | NCs | *P* | Cs | NCs | *P* | Cs | NCs | *P* | Cs | NCs | *P* |
| Superior fossa | −0.30 (1.03) | −0.68 (0.74) | .142 | 0.77 (0.96) | 0.42 (0.77) | .292 | −0.11 (0.48) | −0.01 (0.34) | .550 | 1.55 (0.62) | 1.14 (0.75) | .156 |
| Anterior fossa | −0.35 (0.60) | −0.14 (0.70) | .332 | 0.94 (0.81) | 0.43 (0.75) | .433 | 0.09 (0.32) | 0.15 (0.31) | .616 | 1.36 (0.47) | 1.00 (0.56) | .115 |
| Posterior fossa | −0.36 (0.72) | −0.69 (0.67) | .068 | 0.74 (1.04) | 0.51 (0.77) | .115 | 0.08 (0.27) | 0.16 (0.36) | .565 | 1.43 (0.46) | 1.19 (0.68) | .236 |
| Superior condyle | −0.82 (0.92) | −0.77 (0.80) | .894 | 0.88 (0.83) | 0.68 (1.37) | .761 | −0.28 (0.49) | −0.16 (0.65) | .527 | 1.66 (0.67) | 1.70 (0.99) | .894 |
| Lateral condyle | −1.35 (105) | −1.29 (0.82) | .840 | 1.11 (0.85) | 0.59 (0.71) | .053 | 0.28 (1.16) | 0.11 (0.82) | .563 | 2.22 (1.01) | 1.85 (0.74) | .133 |
| Medial condyle | −0.95 (0.97) | −1.02 (0.69) | .825 | 0.51 (0.43) | 0.25 (0.76) | .027* | 0.35 (1.28) | −0.10 (0.92) | .430 | 1.72 (0.98) | 1.53 (0.76) | .525 |
| Incisal L1 | 0.16 (2.06) | −0.08 (1.87) | .349 | −0.69 (0.93) | −0.59 (0.88) | .455 | 2.16 (2.97) | 1.97 (3.17) | .260 | 3.83 (1.89) | 3.76 (1.87) | .637 |
| Apical L1 | −1.16 (2.14) | −1.14 (2.26) | .910 | −0.55 (1.13) | −0.32 (1.11) | .371 | −1.56 (2.72) | 1.46 (2.77) | .706 | 3.49 (2.14) | 3.64 (1.83) | .569 |
| Mesiobuccal cusp L6 | 0.25 (1.28) | 0.18 (1.39) | .791 | 0.42 (1.19) | −0.27 (1.19) | .174 | 2.58 (2.43) | 2.26 (2.16) | .209 | 3.61 (1.44) | 3.25 (1.53) | .068 |
| Gonion | −2.19 (2.97) | −2.53 (2.67) | .485 | 0.97 (0.70) | 0.82 (1.27) | .702 | 1.32 (1.67) | 1.35 (2.12) | .962 | 3.76 (2.23) | 4.09 (2.12) | .325 |

[a] Cs indicates cleft side; NCs, noncleft side.
* Statistically significant.

could also be influenced by normal growth and bone remodeling or resorption. The methodology applied in this study enabled 3-D assessment of mandibular linear and rotational displacements after BAMP therapy, including assessment of symmetry of mandibular changes. Previous studies have shown the accuracy and reliability of the voxel-based registration[17,19,20] and measurements based on 3-D surface images.[21,22] After a learning curve of 6 months, the methodology applied in this study required approximately 15 hours per patient. Previous studies with BAMP therapy in patients without oral cleft showed a backward and downward displacement of the mandible while maintaining the mandibular plane angle, closure of the gonial angle, and backward displacement of the GF.[12]

## Linear Changes

The GF in the CG was displaced posteriorly, laterally, and superiorly, and it showed a slightly smaller amount of 3-D remodeling than did the NCG (Table 4). When the 3-D components of the direction of changes were tested, statistically significant differences among groups were found (Table 4). However, a 0.6-mm difference may not be clinically significant. GF displacement seems to be associated with mandibular displacement, since the condyle showed a similar pattern of displacement. These results are in accordance with a previous study using BAMP therapy in noncleft patients, which found a posterior remodeling of GF anterior (1.30–1.47 mm)[12] and posterior (1.30–1.39 mm) eminences.[12]

The condyle was displaced posteriorly, laterally, and superiorly in the CG, while it displaced posteriorly, laterally, and inferiorly in the NCG (Table 4). The difference in the vertical direction was not statistically significant. The displacement found in this study corroborates the posterior displacement of the condyle previously found with the maxillary protraction therapy in noncleft patients.[7,12] The gonial landmark also showed a posterior, lateral, and inferior displacement in both groups, suggesting that the whole ramus was displaced backward, also as described in the literature.[12] Even though statistically significant differences were found in median structures (Point B and Incisal L1) for mediolateral displacement, it may not be clinically relevant (Table 4).

When comparing Cs and NCs, we found that only lateral displacement of the medial pole of the condyle on the Cs was significantly greater than the contralateral (Table 5). Even though the lateral pole did not show a statistically significant difference, it did show a greater lateral displacement on the Cs. This asymmetry might have resulted from the slight difference in the elastic direction between Cs and NCs. The miniplate was usually placed more anteriorly in the lesser segment, determining a more vertical elastic vector at this side. Another hypothesis is that the Cs condyle displaces laterally as a counterpart of a greater lateral movement at zygoma on the Cs after BAMP therapy. This correlation is in accordance with previous findings showing that the mandible follows the deviations in maxillary asymmetry of CLP patients.[23]

## Angular Changes

In an anterior view, the intercondylar line showed a significant difference between groups, with a CCW roll

**Table 6** Descriptive and Statistical Analyses of the Comparison of Angular Measurements (T2–T1) Between CG and NCG[a]

| | Yaw (°) | | Roll (°) | | Pitch (°) | |
|---|---|---|---|---|---|---|
| | CG | NCG | CG | NCG | CG | NCG |
| Condylar line | −0.16 (0.57) | 0.08 (0.67) | −0.13 (0.35) | 0.21 (0.46) | | |
| | $P = .274$ | | $P = .021$* | | | |
| Intermolar line | −0.13 (0.88) | −0.21 (1.16) | 0.69 (0.88) | 0.17 (0.93) | | |
| | $P = .811$ | | $P = .113$ | | | |
| Occlusal line | | | | | −1.10 (2.92) | −2.03 (2.31) |
| | | | | | $P = .351$ | |
| Co-Me | | | | | 0.90 (1.92) | 0.08 (1.54) |
| | | | | | $P = .212$ | |

[a] CG indicates cleft group; NCG, noncleft group.
* Statistically significant.

in the CG and a CW roll in the NCG. This difference was not clinically relevant (Table 6). These asymmetrical displacements of the mandible are in accordance with previous findings showing an asymmetrical growth of the mandible following the asymmetric maxilla, indicating an equivalent growth of maxilla and mandible in patients with UCLP.[23]

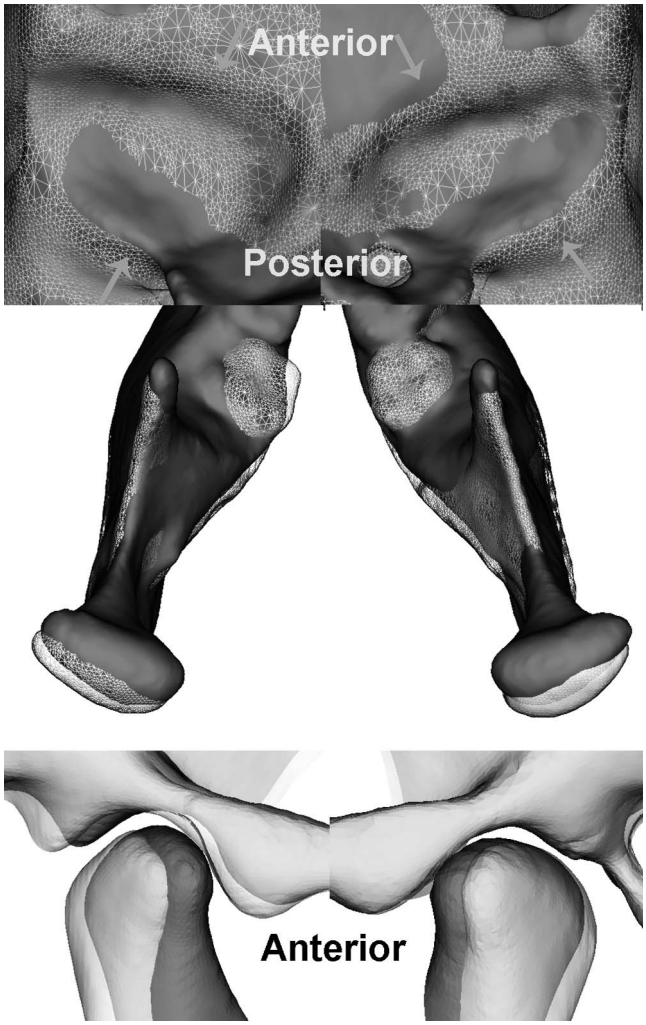


**Figure 4.** Semitransparency superimposition of the fossa, condyle, and temporomandibular changes of a patient of the CG: (a) inferior view of the GF; (b) superior view of the condyle; (c) lateral view of the GF and condyles. T1: red; T2: semitransparent white mesh.

Despite the mandibular growth, the backward and downward displacement of the mandible contributed to orthopedic correction of the Class III malocclusion by masking the mandibular corpus elongation and thereby favoring an improvement in facial convexity and overjet correction after treatment. In the lateral view, the Co-Me line showed a similar CW pitch rotation between the CG and NCG groups, corroborating previous findings.[24] The occlusal line showed a similar slight counterclockwise rotation of both groups, corroborating previous findings.[25] Considering that most of the patients with UCLP show a vertical pattern of growth with reduced ramal height, more obtuse gonial angle, and increased lower anterior facial height,[2] the small amount of clockwise mandibular rotation favored the esthetic treatment outcome (Table 6).

One limitation of this study was the different ethnical backgrounds of the CGs and NCGs. However, the treatment outcomes were similar regardless of the different ethnic origins of the samples. Another limitation of the study was the time interval between the T1 and T2 CBCT scans. The extra 6 months of treatment are related to the learning curve of adapting the protocol of intermaxillary elastic forces in the cleft patients.

The symmetrical GF remodeling may suggest better stability of the mandibular displacement. However, future studies using mandibular regional superimposition should be done to verify the short- and long-term mandibular condylar remodeling pattern to assess growth modification.

## CONCLUSIONS

- BAMP therapy produced significantly smaller 3-D displacement in cleft patients regardless of the direction of the 3-D changes: anteroposterior, mediolateral, and inferior-superior.

- Overall mandibular linear and angular rotational displacements were similar in patients with and without UCLP.
- Despite the presence of a unilateral cleft, most of the mandibular changes were symmetrical in the CG.

## ACKNOWLEDGMENT

The authors would like to acknowledge the FAPESP (São Paulo Research Foundation / n° 2013/17596-3, 2013/19880-0, and 2014/11206-1) for their financial support.

## REFERENCES

1. Semb G. A study of facial growth in patients with unilateral cleft lip and palate treated by the Oslo CLP Team. *Cleft Palate Craniofac J*. 1991;28:1–21; discussion 46–28.
2. Graber TM. A cephalometric analysis of the developmental pattern and facial morphology in cleft palate. *Angle Orthod*. 1949;19:91–100.
3. Aduss H. Craniofacial growth in complete unilateral cleft lip and palate. *Angle Orthod*. 1971;41:202–213.
4. Silva Filho OG, Corrêa Normando AD, Capelozza Filho L. Mandibular morphology and spatial position in patients with clefts: intrinsic or latrogenic? *Cleft Palate Craniofac J*. 1992;29:369–375.
5. Ross RB, Johnston MC. The effect of early orthodontic treatment on facial growth in cleft lip and palate. *Cleft Palate J*. 1967;4:157–164.
6. Ross RB. The clinical implications of facial growth in cleft lip and palate. *Cleft Palate J*. 1970;7:37–47.
7. Baccetti T, Franchi L, McNamara JA, Jr. Treatment and posttreatment craniofacial changes after rapid maxillary expansion and facemask therapy. *Am J Orthod Dentofacial Orthop*. 2000;118:404–413.
8. De Clerck HJ, Cornelis MA, Cevidanes LH, et al. Orthopedic traction of the maxilla with miniplates: a new perspective for treatment of midface deficiency. *J Oral Maxillofac Surg*. 2009;67:2123–2129.
9. Cevidanes L, Baccetti T, Franchi L, et al. Comparison of two protocols for maxillary protraction: bone anchors versus face mask with rapid maxillary expansion. *Angle Orthod*. 2010;80:799–806.
10. Ruf S, Pancherz H. Temporomandibular joint remodeling in adolescents and young adults during Herbst treatment: a prospective longitudinal magnetic resonance imaging and cephalometric radiographic investigation. *Am J Orthod Dentofacial Orthop*. 1999;115:607–618.
11. Janzen EK, Bluher JA. The cephalometric, anatomic, and histologic changes in Macaca mulatta after application of a continuous-acting retraction force on the mandible. *Am J Orthod*. 1965;51:823–855.
12. De Clerck H, Nguyen T, de Paula LK, et al. Three-dimensional assessment of mandibular and glenoid fossa changes after bone-anchored Class III intermaxillary traction. *Am J Orthod Dentofacial Orthop*. 2012;142:25–31.
13. Mars M, Plint DA, Houston WJ, et al. The Goslon Yardstick: a new system of assessing dental arch relationships in children with unilateral clefts of the lip and palate. *Cleft Palate J*. 1987;24:314–322.
14. Nguyen T, Cevidanes L, Cornelis MA, et al. Three-dimensional assessment of maxillary changes associated with bone anchored maxillary protraction. *Am J Orthod Dentofacial Orthop*. 2011;140:790–798.
15. Yushkevich PA, Piven J, Hazlett HC, et al. User-guided 3D active contour segmentation of anatomical structures: significantly improved efficiency and reliability. *Neuroimage*. 2006;31:1116–1128.
16. Fedorov A, Beichel R, Kalpathy-Cramer J, et al. 3D Slicer as an image computing platform for the Quantitative Imaging Network. *Magn Reson Imaging*. 2012;30:1323–1341.
17. Ruellas AC, Tonello C, Gomes LR, et al. Common 3-dimensional coordinate system for assessment of directional changes. *Am J Orthod Dentofacial Orthop*. 2016;149:645–656.
18. Cevidanes LH, Heymann G, Cornelis MA, et al. Superimposition of 3-dimensional cone-beam computed tomography models of growing patients. *Am J Orthod Dentofacial Orthop*. 2009;136:94–99.
19. Ruellas AC, Huanca Ghislanzoni LT, Gomes MR, et al. Comparison and reproducibility of 2 regions of reference for maxillary regional registration with cone-beam computed tomography. *Am J Orthod Dentofacial Orthop*. 2016;149:533–542.
20. Ruellas AC, Yatabe MS, Souki BQ, et al. 3D mandibular superimposition: comparison of regions of reference for voxel-based registration. *PLoS One*. 2016;11:e0157625.
21. Berco M, Rigali PH, Jr., Miner RM, et al. Accuracy and reliability of linear cephalometric measurements from cone-beam computed tomography scans of a dry human skull. *Am J Orthod Dentofacial Orthop*. 2009;136:17 e11–e19; discussion 17–18.
22. El-Beialy AR, Fayed MS, El-Bialy AM, et al. Accuracy and reliability of cone-beam computed tomography measurements: influence of head orientation. *Am J Orthod Dentofacial Orthop*. 2011;140:157–165.
23. Laspos CP, Kyrkanides S, Tallents RH, et al. Mandibular asymmetry in noncleft and unilateral cleft lip and palate individuals. *Cleft Palate Craniofac J*. 1997;34:410–416.
24. Tindlund RS, Rygh P. Maxillary protraction: different effects on facial morphology in unilateral and bilateral cleft lip and palate patients. *Cleft Palate Craniofac J*. 1993;30:208–221.
25. Baek SH, Kim KW, Choi JY. New treatment modality for maxillary hypoplasia in cleft patients. Protraction facemask with miniplate anchorage. *Angle Orthod*. 2010;80:783–791.